



Modelling the fine-scale spatiotemporal pattern of urban heat island effect using land use regression approach in a megacity

Yuan Shi ^{a,*}, Lutz Katzschner ^b, Edward Ng ^{a,c,d}

^a School of Architecture, The Chinese University of Hong Kong, Shatin, NT, Hong Kong, China

^b Department of Environmental Meteorology, Faculty of Architecture and Planning, University of Kassel, Germany

^c Institute of Environment, Energy and Sustainability (IEES), The Chinese University of Hong Kong, Shatin, NT, Hong Kong, China

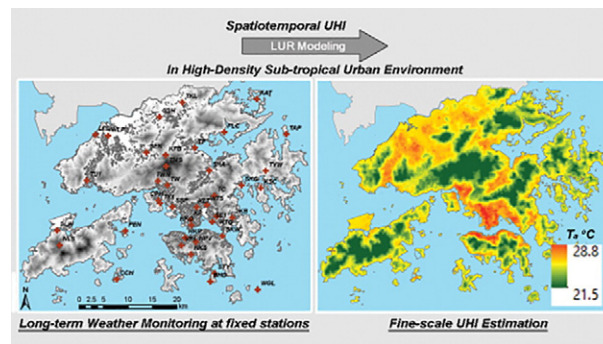
^d Institute Of Future Cities (IOFC), The Chinese University of Hong Kong, Shatin, NT, Hong Kong, China



HIGHLIGHT

- Applying LUR modelling method for fine-scale spatiotemporal UHI estimation
- Adopting LUR in subtropical high-density urban environment
- 10 LUR models were developed for daytime and nighttime UHI in different seasons.
- Moderately good performance (R^2 of 0.6–0.7) were achieved in resultant models.
- UHI are largely determined by the LU/LC and urban geomorphometry.

GRAPHICAL ABSTRACT



ARTICLE INFO

Article history:

Received 2 July 2017

Received in revised form 14 August 2017

Accepted 25 August 2017

Available online 31 October 2017

Editor: D. Barcelo

Keywords:

Urban heat island
Land use regression
Spatiotemporal pattern
Urban geomorphometry

ABSTRACT

Urban heat island (UHI) effect significantly raises the health burden and building energy consumption in the high-density urban environment of Hong Kong. A better understanding of the spatiotemporal pattern of UHI is essential to health risk assessments and energy consumption management but challenging in a high-density environment due to the sparsely distributed meteorological stations and the highly diverse urban features. In this study, we modelled the spatiotemporal pattern of UHI effect using the land use regression (LUR) approach in geographic information system with meteorological records of the recent 4 years (2013–2016), sounding data and geographic predictors in Hong Kong. A total of 224 predictor variables were calculated and involved in model development. As a result, a total of 10 models were developed (daytime and nighttime, four seasons and annual average). As expected, meteorological records (*CLD*, *Spd*, *MSLP*) and sounding indices (*KINX*, *CAPV* and *SHOW*) are temporally correlated with UHI at high significance levels. On the top of the resultant LUR models, the influential spatial predictors of UHI with regression coefficients and their critical buffer width were also identified for the high-density urban scenario of Hong Kong. The study results indicate that the spatial pattern of UHI is largely determined by the LU/LC (*RES1500*, *FVC500*) and urban geomorphometry (\bar{h} , *BVD*, $\bar{\lambda}_F$, Ψ_{sky} and z_0) in a high-density built environment, especially during nighttime. The resultant models could be adopted to enrich the current urban design guideline and help with the UHI mitigation.

© 2017 Elsevier B.V. All rights reserved.

* Corresponding author at: Rm505, AIT Building, School of Architecture, The Chinese University of Hong Kong, Shatin, NT, Hong Kong, China.
E-mail address: shiyuan@cuhk.edu.hk (Y. Shi).

Nomenclature¹

Symbols and abbreviations

A.A.D.T	Annual Average Daily Traffic
ADDRESS	A Distance Decay REgression Selection Strategy
A_F	Total frontal area of all buildings in the urban lot along with the wind direction
AICc	Akaike information criterion
A_p	Building footprint area
A_T	The area of a certain urban lot
AWSS	automatic weather stations
BIC	Bayesian information criterion
C&SD	Hong Kong Census and Statistics Department
C_{Dh}	drag coefficient
d	The radius of the hemisphere circle for SVF calculation
DEM	digital elevation model
GIS	geographical information system
h	building height
HKO	Hong Kong Observatory
HKPSG	Hong Kong Planning Standards and Guidelines
HKTD	Hong Kong Transport Department
ISA	impervious surface area ratio
K	Kármán's constant
LCZ	local climate zone
LOOCV	leave-one-out cross-validation
LST	land surface temperature
LU/LC	Land use and land cover
LUR	Land use regression
MLR	multiple linear regression
NDBI	Normalized Difference Building Index
NDVI	Normalized Difference Vegetation Index
$P_{(\theta)}$	the probability of wind direction θ .
PlanD	Hong Kong Planning Department
p-Value	significant level
r	Coefficient of correlation
R^2	coefficient of determination
RMSE	root-mean-square error
RS	Remote sensing
SB/VC	Street Block/Village Clusters
SUHI	surface urban heat island
UHI	urban heat island
V	total building volume of each district
v, Spd	wind speed (m/s)
Var	regression model predictor
VIF	variance inflation factor
z_0	roughness length
α	slope aspect
α_m, β_n	Slopes of regression model predictors
$\alpha_{r(\theta)}$	The angle between the slope aspect α of a certain location and wind direction θ
β	slope angle
γ	Regression model intercept
ε	residual
θ	wind direction (0–360°)
λ_F, FAI	frontal area index
λ_p	Building coverage ratio
φ	horizon angles
$\Psi_{sky,SVF}$	sky view factor
Φ	azimuth directions

1. Introduction

Over the past few decades, the negative impacts of climate and weather conditions on public health have been identified as an issue of increasing concern (Patz et al., 2005; WHO, 2003). To be more specific, impacts of climate change (especially, the trend of global warming) and the intensifying urban heat island (UHI) effect due to rapid urbanization lead to much more frequent, longer and more severe heatwave events in urban areas (Li and Bou-Zeid, 2013). UHI effect refers to the phenomenon that the ambient air temperature in highly-urbanized areas is higher than the rural area and natural lands (Rizwan et al., 2008). Rapid urbanization processes change the natural landscape into highly artificial environments, which change the land surface geomorphometry as well as the thermal properties (e.g. emissivity, permeability). As a result, the radiation balance in the urbanized area is greatly different from the neighboring rural area. Urbanization also introduces a large amount of anthropogenic heat which further exacerbates the UHI intensity (measured by the air temperature difference between urban and rural area) (Taha, 1997). The subsequent negative impacts on public health have been identified as serious threats to public health and have raised concerns.

A number of studies have proved strong associations between the increases in health risks and UHI effect with intensified heat waves, both in the long and short term, worldwide (Anderson and Bell, 2009; Buechley et al., 1972; Clarke, 1972; Meehl and Tebaldi, 2004) and locally in Hong Kong (Goggins et al., 2012; Yan, 2000). It has been found that a 1 °C increase in air temperature of 29 °C is associated with a 4% increase in mortality in those areas of Hong Kong with high UHI intensity. In contrast, the corresponding mortality increase in low UHI intensity areas is <1% (Goggins et al., 2012). This finding indicates the UHI effect could lead to a much higher local health burden under the same regional weather background. The above implies that a better understanding and more detailed information of the spatiotemporal pattern of UHI are urgently needed for urban environmental management and heat-related health risk assessment. For instance, local scholars emphasize that a hot weather warning system might be useful to reduce elderly mortality (Chau et al., 2009). The detailed information of the spatiotemporal pattern of UHI will play an important role in that.

In Hong Kong, hourly weather conditions are currently observed and recorded by a well-equipped local monitoring network maintained by the Hong Kong Observatory (HKO). Currently, it contains 85 well-instrumented automatic weather stations (AWSSs). In this present study, the data of ambient air temperature are obtained from 42 AWSSs of this network (Fig. 2). The local meteorological records provide fine temporal resolution for UHI studies. However, the real challenge of a local UHI study is that, Hong Kong has a total land area of around 1100 km² and with extremely heterogeneous urban settings (including but not limited to topography, land coverage, natural landscape, land use, building form and population distribution, etc.). This heterogeneity results in large ambient air temperature variations between different locations of the city, which cannot be effectively observed by the sparsely distributed meteorological stations. This consequently introduces the issue of using the meteorological records from the closest AWSSs. The distance between the site and the AWS may lead to uncertainties and even errors in the mapping of the spatiotemporal pattern of the UHI and further investigation of heat-related health risks at the community level. Moreover, the identification of hotspots and problematic areas of heat-related health risks will be difficult if only the local monitoring network is used.

Remote sensing (RS) satellite-based methods are also popularly used to explore the spatial structure of UHI (Gallo et al., 1995; Tomlinson et al., 2011), because these methods provide sufficient spatial information at a relatively fine resolution (90–120 m) (Liu and Zhang, 2011; Nichol and Wong, 2005). However, the main issue of using satellite images is that the retrieved UHI measurements are based on land surface temperature (LST) not the ambient air

¹ The abbreviations of all land use variables/predictors have been included in Table 1, thus not be included in this nomenclature.

temperature. It is a known fact that the diurnal cycle of atmospheric UHI and surface UHI (SUHI) are considerably different (Roth et al., 1989). The atmospheric UHI is larger during nighttime while the SUHI is larger during the daytime. Using SUHI for heat-related health risk assessment may introduce estimation error. Other vegetation and land use/land cover indicators, such as Normalized Difference Vegetation Index (NDVI), Normalized Difference Building Index (NDBI) and impervious surface area ratio (ISA), are also commonly retrieved and used for UHI estimation (Zhang et al., 2009; Zhou et al., 2014b). However, the use of these indexes alone may be still insufficient for UHI estimation in Hong Kong due to the cloudy weather and the occlusion issue among high-rise buildings.

To overcome the above limitations of RS-based UHI studies, an attempt has been made to quantify the UHI intensity by classifying the near surrounding of a very limited number of weather stations (17 stations) using the concept of local climate zone (LCZ) classification with long-term monitored data (Siu and Hart, 2013). Attempts have been made to quantify the correlations between UHI and urban surface geometry with statistical algorithm as well (Svensson, 2004; Unger, 2004). In Hong Kong, a significant correlation has been found between the intra-urban air temperature difference and a surface-geometrical parameter – sky view factor (SVF) (Chen et al., 2012), which means that the incorporation of surface geometry as predictors will help improve the accuracy of UHI estimation. However, there are still some general limitations of the inner LCZ variability and the issues of unclassifiable areas due to the extremely heterogeneous city form (Leconte et al., 2015). In some cases, the results are also sensitive to the spatial scale/resolution used for data analysis (Kotharkar and Bagade, 2007). Moreover, it can be observed that the detailed methods of data processing vary between different studies despite the standardization efforts of LCZ. Therefore, a standardized method is necessary as a supplement to avoid the current limitations of unclassifiable areas and also the differentiation in data processing among different studies.

Land Use Regression (LUR) is a popularly used and standardized statistical method in the estimation of spatial variation of environmental exposure at a fine scale and has been widely adopted in public health studies (Hoek et al., 2008; Ryan and LeMasters, 2007; Xie et al., 2011). LUR estimates the environmental exposure level of locations/individuals in a study area by treating them as the response variable of a multiple linear regression model (MLR) of several explanatory variables resulting from geographical predictors and urban indices (such as land use, traffics and population) in a series of buffers of the receivers' location. Using statistical algorithms in geographical information system (GIS), LUR can accurately estimate the long-term averaged environmental exposure level in unmonitored areas based on existing monitoring locations. An attempt has been made in applying LUR method in the investigation of the effect of land use on temperature during heat waves (Zhou et al., 2014a). Furthermore, recent LUR research have focused on developing temporal-resolved LUR models (Kloog et al., 2012; Saraswat et al., 2013). These temporal-resolved models allow for a series of mappings of spatiotemporally varying environmental exposure level at a finer spatial resolution compared to the RS results (Hoek et al., 2008). Therefore, temporal-resolved LUR models could be helpful in the process of health risk assessment and further environmental policy-making.

The objective of this present study is to estimate the spatiotemporal variation of UHI for high-density Hong Kong for the purpose of providing a good reference for heat-related health risk assessment. In Hong Kong, spatially varying urban surface characteristics (both the natural landscape and artificial environment) significantly modifies the local meteorological conditions, and subsequently affects the intraurban UHI pattern. Moreover, the intraurban air temperature difference is also affected by the non-uniformly distributed local anthropogenic heat sources. In this study, for the first time, we introduce the LUR method to estimate the spatiotemporal UHI in Hong Kong by incorporating LUR modelling with a comprehensive set of geographic/meteorological predictors.

2. Materials and methods

Traditionally, UHI is defined as the air temperature difference between urban and rural areas. However, it is difficult to define the specific terms of “urban” and “rural” in the spatially varied and unique urban context of Hong Kong (Siu and Hart, 2013). Assessing the heat-related health risk need as detailed as possible spatiotemporal information of UHI rather than a simple value of air temperature difference between urban and rural areas. Therefore, in this study, air temperature measurement from the HKO AWSs network over the years of 2013–2016 are used as the proxy for investigating the UHI effect, as such used as the response variable for spatiotemporal LUR modelling. A comprehensive set of geographic/meteorological predictors (land cover, urban indices and meteorological sounding data) were selected as explanatory variables and calculated in GIS by following the buffer-based analysis process of LUR method (Ryan and LeMasters, 2007). After developing the LUR model, the spatiotemporal distribution of air temperature can be mapped for UHI investigation and also adopted as the basis for public health assessment. Fig. 1 shows the workflow of the LUR approach used in this present study.

2.1. Response variables - air temperature measurements

LUR studies typically use an environmental exposure sample set of 20–100 fixed reference points within the study area (Hoek et al., 2008). As mentioned, hourly air temperature measurements at 42 AWSs of HKO meteorological monitoring network over Hong Kong are available for this study which is much more than a previous study (17 stations involved only) (Siu and Hart, 2013). Hourly meteorological records of the years 2013–2016 were obtained from HKO. Daily air temperature were calculated in terms of daytime and nighttime average to separately develop models so that the difference of UHI pattern between day and night can be observed. The annual and seasonal averages (Spring - Mar to Apr; summer - May to Aug; Fall - Sep to Nov; winter - Dec to Feb (Chin, 1986)) of air temperature are also calculated to understand the seasonal difference of the UHI pattern. Figs. 3 and 4 show the data plot of daily average air temperature of different AWSs (by grouping the data by seasonal periods and separating them in daytime and nighttime). The above data are used as response variables to develop the LUR models. A total of ten models will be developed (daytime and nighttime, four seasons and annual average).

2.2. Weather records and meteorological variables as temporal predictors

Besides the hourly records of air temperature (T_a), other available hourly weather data include wind speed (Spd), rainfall (Rf), mean sea level pressure ($MSLP$) and cloudiness (CLD) were also requested from HKO. Rainfall measurements are not available for a few of those AWSs. Therefore, observatory data were assigned to the nearest AWS for those with no available records. A total of 18 sounding indices were also used in this study as model predictors (Table 1) because the atmospheric stability is also closely related to the spatial pattern and intensity of UHI (Lee, 1979; Oke, 1982). Relative humidity (RH) was not used as a predictor variable because it is inherently correlated with T_a .

2.3. Geographic variables as spatial predictors

A total of five categories of data sets were prepared as the geographic predictors for the LUR modelling of UHI in this present study. They are (1) land use distribution, (2) population distribution, (3) traffic volume, (4) natural geography and (5) urban surface geomorphometry. The ambient T_a is jointly determined by the local condition within a small scale neighborhood and the regional background condition of a larger area. To consider both the local and regional effects. All predictors were calculated in a series of varied buffer widths (range from 50 m to 5000 m) for each AWS (Table 1).

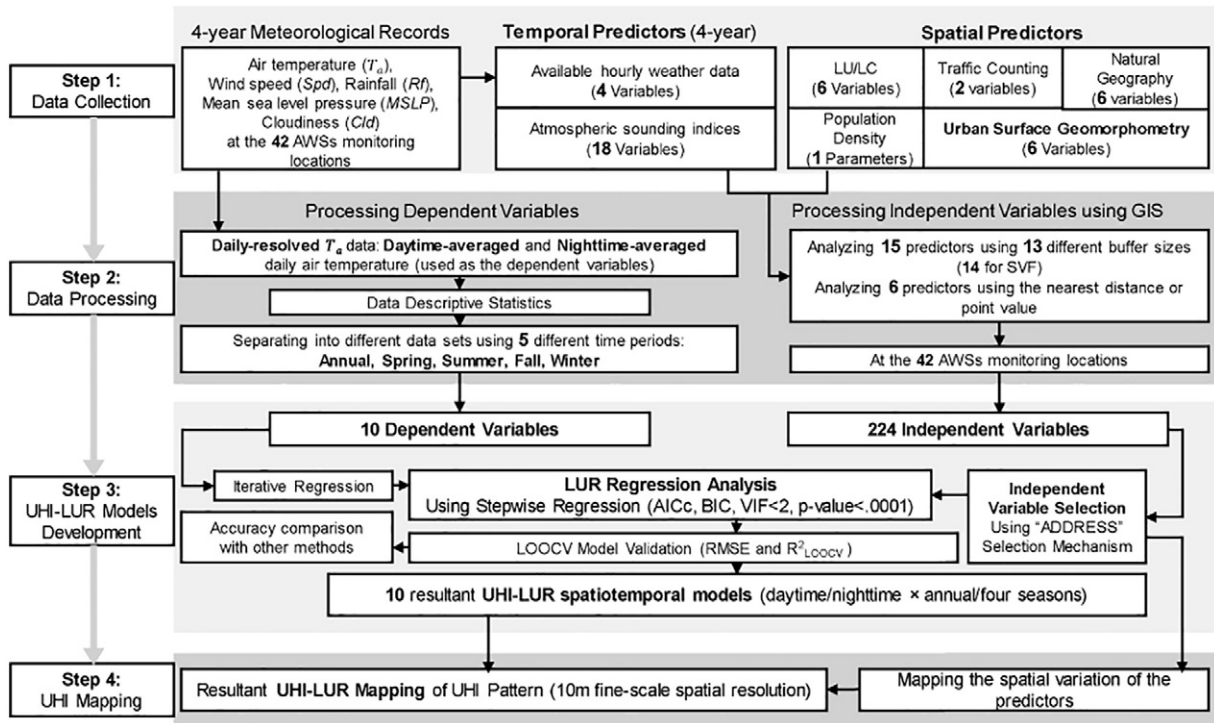


Fig. 1. The workflow chart of this present LUR modelling study.

2.3.1. Land use and land cover (LU/LC)

Land distribution as an influential factor of UHI (Bottyán and Unger, 2002; Oke, 1982) has been used for regional/urban climatic mapping (Katzschner and Müller, 2008), thus adopted as the predictors of the LUR modelling in this study. The land use distribution of Hong Kong was requested from the Hong Kong Planning Department

(PlanD). Based on the literature of previous LUR studies (Hoek et al., 2008), the complex land use types of Hong Kong was reclassified as the following types: Residential area (RES); Commercial area (COM); Industrial area (IND); Government area (GOV) and Open space area (OPN). Using buffering analysis, we calculated the total area (measured in the unit of m²) of each reclassified land use type in the buffers for

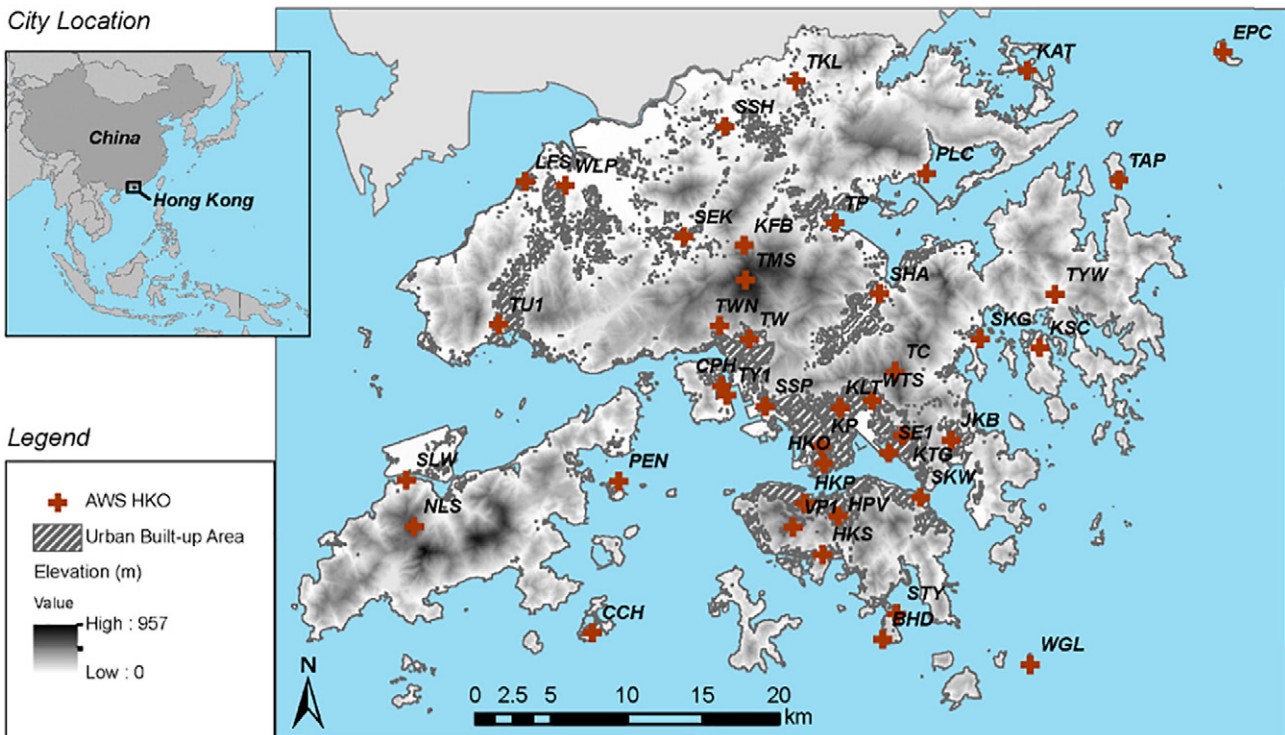


Fig. 2. The locations of 42 available HKO AWSs in the local weather observation network of Hong Kong.

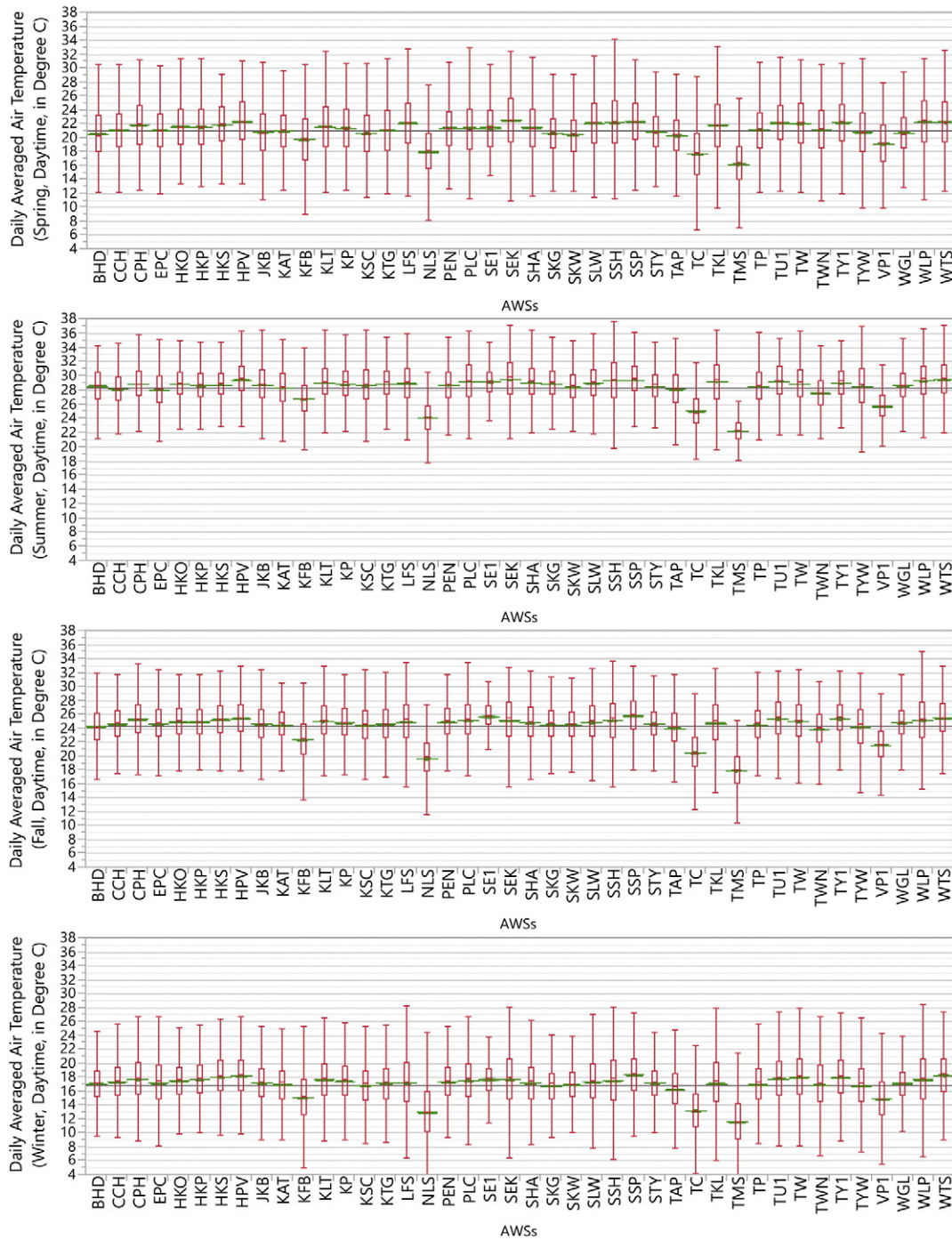


Fig. 3. Seasonal data plot of daily averaged daytime air temperature observations.

each AWS as a predictor variable. Fractional vegetation cover (FVC) was also used as a spatial predictor variable of UHI because it depicts the spatial coverage of vegetation and also implies the fraction of pervious and impervious surface.

2.3.2. Population distribution

The population distribution has been commonly investigated in UHI studies (Oke, 1973) because it is a major factor of profiling anthropogenic heating in urban areas (Fan and Sailor, 2005; Sailor and Lu, 2004). In this present study, the most recent population census data of the year 2011 is obtained from Hong Kong Census and Statistics Department (C&SD). The population distribution was mapped using the digital boundary of Street Block/Village Clusters (SB/VC, obtained from PlanD,

which is a standard planning level of Hong Kong) for calculating the population density (people/km²) in the buffers of each AWS.

2.3.3. Traffic counting

UHI is exacerbated by the anthropogenic heating from vehicles (Yuan and Bauer, 2007). Therefore, it is necessary to examine the possible impact of urban traffic in a UHI study. The number of vehicles in different road segments in Hong Kong is counted at >800 counting stations and averaged to obtain the Annual Average Daily Traffic (A.A.D.T) data (HKTD, 2016). The A.A.D.T data and spatial distribution of the counting stations are available at the Hong Kong Transport Department (HKTD) in their “Annual Traffic Census”. In this study, to map the spatial distribution of the traffic volume, the A.A.D.T data were aggregated as a raster

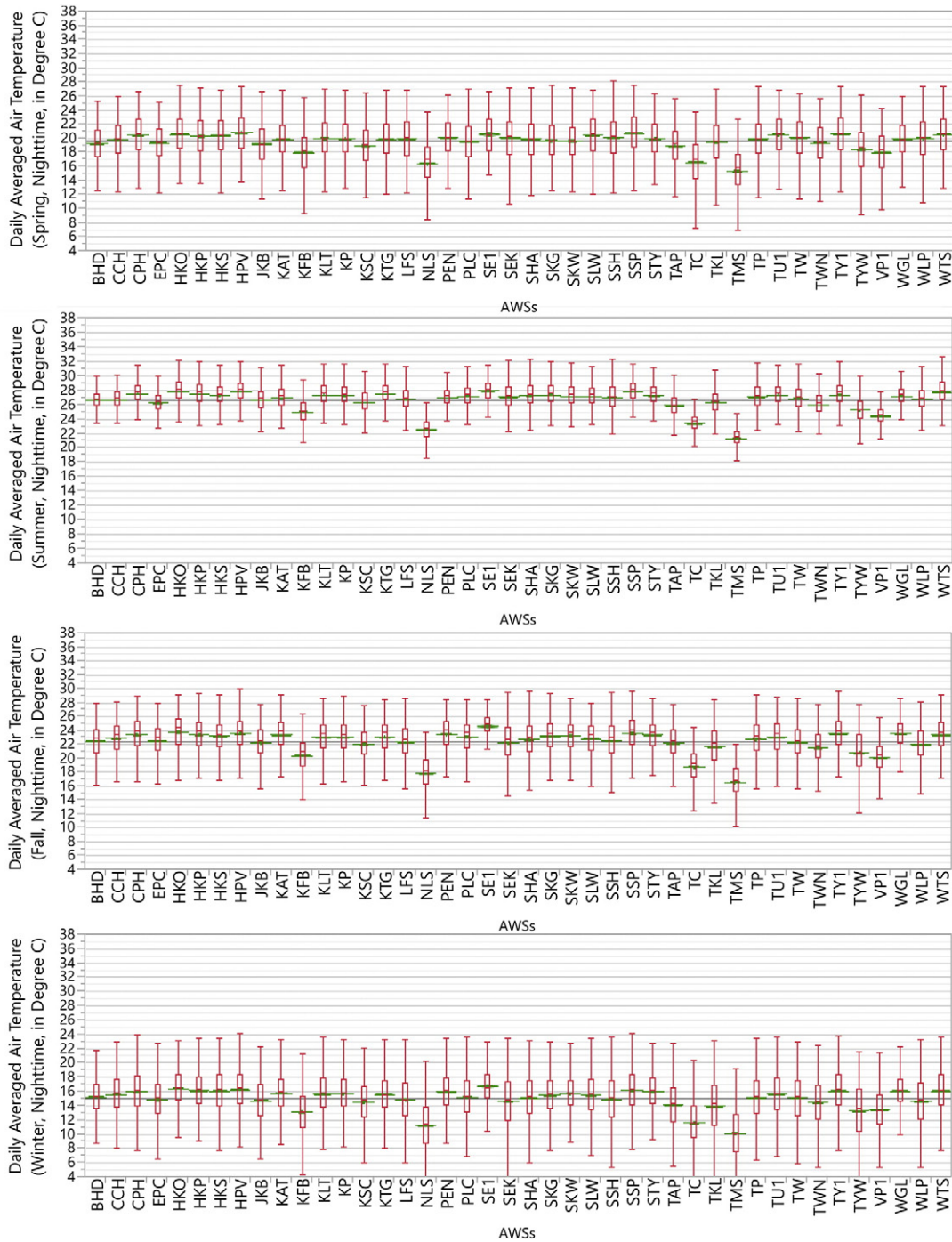


Fig. 4. Seasonal data plot of daily averaged nighttime air temperature observations.

data layer in GIS using a grid system with a spatial resolution of 100 m (corresponding to the smallest buffer size used in this study which is 50 m) based on the road network. The traffic volume of public transport vehicles and private/government vehicles were mapped separately as two data layers in order to differentiate waste heat sources of different types of vehicles. The traffic volume within the neighboring area of each AWS was then calculated by using buffering analysis.

2.3.4. Natural geography and landscape

A set of commonly-used variables was selected as the predictors to profile the surrounding natural geography of AWSs: x coordinate, y coordinate, altitude, nearest distance to waterfront, distance to city parks,

distance to country parks. All spatial data were projected to the HK1980 coordinate system.

2.3.5. Urban surface geomorphometry

Densely-built urban forms significantly change the aerodynamic and thermal properties of the ground surface, and hence alter the wind field and radiation/energy balance near the ground surface and result in considerable urban microclimatic variation (Arnfield, 2003). Urban form and building density differences result in spatial variability in the intraurban air temperature (Givoni, 1998). Therefore, the use of those commonly-used land use variables mentioned above alone may not be sufficient in the investigation of the intraurban air temperature differences in the highly varied urban environment of Hong Kong. To consider

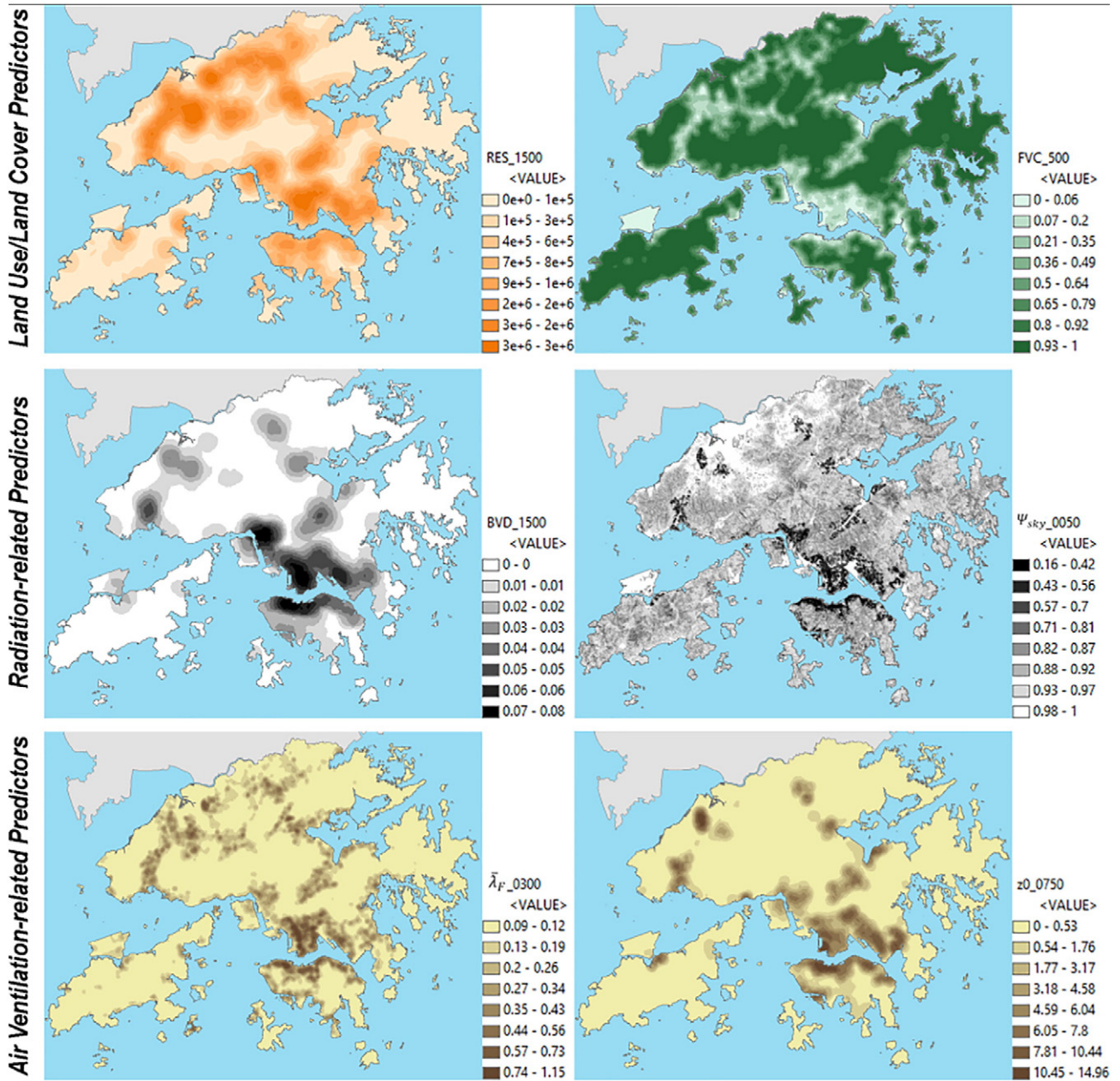


Fig. 5. Example mapping of spatial distribution of spatial predictors.

the urban geomorphometric variability and its influence on the spatial pattern of UHI in a high-density urban environment, a set of urban surface geomorphometric parameters was calculated and used as predictor variables in LUR modelling. They are the mean building height (\bar{h}), building ground coverage ratio (λ_p), building volume density (BVD), sky view factors (Ψ_{sky}), weighted frontal area index based on the probability of wind directions ($\bar{\lambda}_F$), urban surface roughness length (z_0). Among these parameters, \bar{h} and λ_p are the most basic parameters of describing the geometrical characteristics of building bulks:

$$\bar{h} = \frac{1}{n} \sum_{i=1}^n h_i$$

$$\lambda_p = \left(\sum_{i=1}^n A_{pi} \right) / A_T$$

where \bar{h} is the averaged building height of a district. n is the total number of buildings in the district. h_i is the height of the building i . A_T is the

area of the district. A_{pi} is the footprint area of the building i . Building bulks absorb the shortwave solar radiation during the daytime such that the volume of the buildings determines the capacity of heat storage. During the nighttime, a larger building volume blocks more longwave radiation (released by the buildings) than an open area, and consequently traps more heat within the city. Therefore, a higher the building volume density leads to a larger heat capacity (Ng and Ren, 2015). BVD is calculated as follows:

$$V = \sum_{i=1}^n A_{pi} h_i$$

$$BVD_j = V_j / V_{max}$$

where the total building volume of each district in the city is calculated as V . j is the total number of the districts. V_{max} is the highest V among all districts in the city. Ψ_{sky} , as a measure of urban geometry, has been widely used to analyze the intraurban variation for the three decades (Chen et al., 2012; Eliasson, 1990; Hillevi and Deliang, 1999). It was

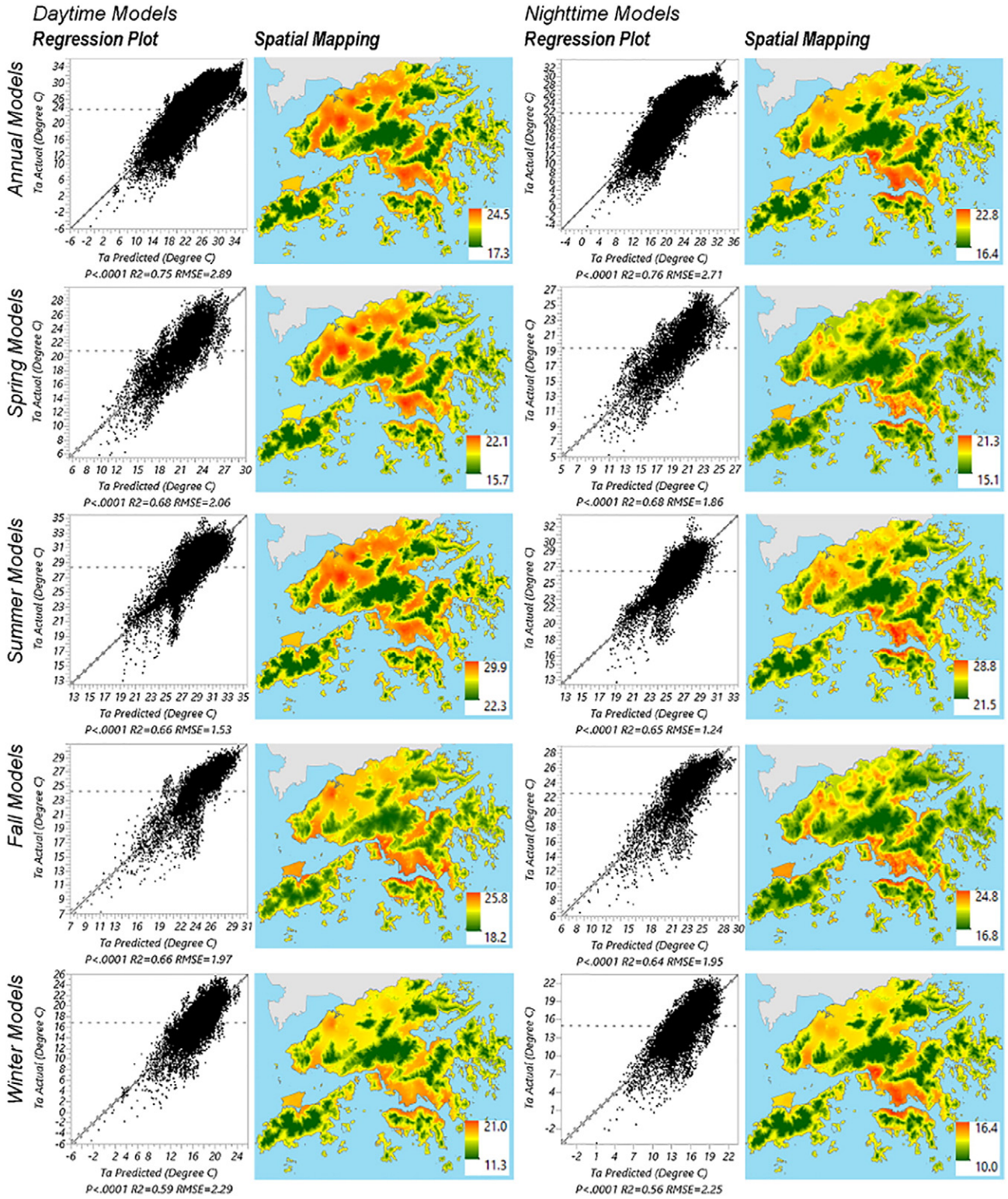


Fig. 6. Regression plot of all resultant models and corresponding spatial mapping of annual/seasonal averaged daytime and nighttime UHI spatial mapping.

calculated by following the formula proposed by Dozier and Frew (1990) using the 1 m-resolution digital elevation model (DEM) of the entire Hong Kong:

$$\Psi_{sky} = \frac{1}{2\pi} \int_0^{2\pi} [\cos\beta \cos^2\varphi + \sin\beta \cdot \cos(\Phi-\alpha) \cdot (90-\varphi - \sin\varphi \cos\varphi)] d\Phi$$

where the Ψ_{sky} value is calculated for each pixel of the DEM with the corresponding slope aspect α , slope angle β and the horizon angles φ in azimuth directions Φ of the hemisphere circle with a search radius of d . Variables $\bar{\lambda}_F$ and z_0 are related to the conditions of urban ventilation which are influential in the cooling potential as well. It has been proved that the incorporation of $\bar{\lambda}_F$ and z_0 enhances the LUR model performance of air pollution in a high-density scenario (Shi et al., 2017).

Table 1
List of the temporal and spatial predictor variables for LUR modelling of UHI.

Categories	Predictor variables	Unit ^a	Abbreviation
Temporal predictors			
Available hourly weather data (4 variables)	Wind speed (measured at the WGL as the background wind condition)	m/s	Spd
	Rainfall	mm	Rf
	Mean sea level pressure (measured at the location of WGL)	hPa	MSLP
	Cloudiness (measured at the location of HKO)	Oktas	CLD
Atmospheric sounding indices (18 variables)	K index		KINX
	SWEAT index		SWET
	Lifted index		LIFT
	LIFT computed using virtual temperature		LIFV
	Showalter index		SHOW
	Cross totals index		CTOT
	Total totals index		TTOT
	Convective Inhibition	J/kg	CINS
	Mean mixed layer mixing ratio	g/kg	MLMR
	Convective Available Potential Energy	J/kg	CAPE
	CAPE using virtual temperature	J/kg	CAPV
	CINS using virtual temperature	J/kg	CINV
	Bulk Richardson Number		BRCH
	Bulk Richardson Number using CAPV		BRCV
	Mean mixed layer potential temperature	K	MLPT
	Temperature of the Lifted Condensation Level	K	LCLT
	Total precipitable water	mm	PWAT
	Pressure of the Lifted Condensation Level	hPa	LCLP
Spatial predictors			
LU/LC (Total land area within certain buffer width ^b , 6 variables)	Residential use	m ²	RES
	Commercial use	m ²	COM
	Industrial use	m ²	IND
	Government use	m ²	GOV
	Open space	m ²	OPN
	Fractional vegetation cover	% ^d	FVC
Population distribution (1 variables)	Population density	People/km ²	POP
Traffic counting (A.A.D.T, 2 variables) ^c	A.A.D.T of public transport vehicles	Vehicles	AADTPT
	A.A.D.T of private/government vehicles	Vehicles	AADTPG
Natural geography (based on HK1980 coordinate system,6 variables)	Longitude	m	X
	Latitude	m	Y
	Altitude/elevation of the monitoring station	m	Z
	Distance to waterbody	m	<i>d_{water}</i>
	Distance to city parks	m	<i>d_{cityp}</i>
	Distance to country parks	m	<i>d_{countryp}</i>
Urban surface geomorphometry (6 variables)	Mean building height	m	\bar{h}
	Building grounding coverage ratio	%	λ_p
	Building volume density	%	BVD
	Sky view factor ^e	%	Ψ_{sky}
	Weighted frontal area index based on the probability of 16 wind directions		$\bar{\lambda}_F$
	Urban surface roughness length	m	z_0

^a Empty cell means the data of the corresponding variable is a dimensionless number.
^b The buffer width series: 50, 100, 200, 300, 400, 500, 750, 1000, 1500, 2000, 3000, 4000, 5000 m.
^c More details are available at the publicly assessable annual traffic census by HKTD at <http://www.td.gov.hk/>.
^d Data normalization (Percentage value/100). All percentage values were normalized into [0–1].
^e Point Ψ_{sky} value was represent as the Ψ_{sky} within a buffer width of 0 m.

Incorporating these variables could possibly improve the estimation accuracy of T_a under such scenario as well. In this present study, they were calculated based on the local building dataset using following equations:

$$\bar{\lambda}_F = \sum_{\theta=1}^{16} \left[\left(\sum_{i=1}^n A_{Fi(\theta)} \right) / A_T \right] P_{(\theta)}$$

$$z_0 = \left\{ h - h \cdot \lambda_p^{0.6} \right\} \exp \left[- \frac{K}{\sqrt{0.5 \cdot C_{Dh} \cdot \bar{\lambda}_F}} \right]$$

where $A_{Fi(\theta)}$ is the frontal area of building i under the scenario of wind direction θ . $P_{(\theta)}$ is the probability of the scenario of wind direction θ .

C_{Dh} is drag coefficient considered as 0.8. K is the Kármán's constant of 0.4. Fig. 5 shows the spatial distribution of several spatial predictors as examples. We use a 10 m–spatial resolution for the mapping of all urban geomorphometric parameters, which is informative for fine-scale LUR modelling of air temperature variability.

2.4. Statistical modelling and validation methods

The study aims to develop LUR models for the investigation of the UHI spatiotemporal pattern by using spatial and temporal predictors as explanatory variables. Statistical regression modelling was conducted to develop the LUR models for investigating daytime and nighttime UHI spatiotemporal pattern in different seasons. Daytime and nighttime daily averaged T_a were used as the response variables for the model development with those predictor variables listed in Table 1 as

explanatory variables. As commonly used in previous studies, the multiple linear regression (MLR) modelling method was conducted in this study. The structure of a spatiotemporal LUR modelling by using MLR is as follows:

$$T_{ajj} = \alpha_1 \text{Var}_{t1j} + \dots + \alpha_m \text{Var}_{tmj} + \beta_1 \text{Var}_{s1ij} + \dots + \beta_n \text{Var}_{snij} + \gamma + \varepsilon$$

where T_{ajj} is the observed air temperature at the location i on day j . The model includes m temporal predictors and n spatial predictors. $\alpha_1, \dots, \alpha_m$ are the slopes of values of the temporal predictors $\text{Var}_{t1}, \dots, \text{Var}_{tm}$ on day j . β_1, \dots, β_n are the slopes of spatial predictors $\text{Var}_{s1}, \dots, \text{Var}_{sn}$ at the location i on day j . γ is the model intercept and ε is the residual.

2.4.1. Sensitivity test for determining the critical buffer width for spatial variables

Buffering analysis was performed for 15 buffer-based spatial predictors using 13 buffer width. Together with other variables, a total of 224 explanatory variables need to be examined for model development. The optimal spatial scales in the evaluation of the microclimatic impact of different spatial variables are varied. For example, it has been found that the air temperature variation has a higher correlation with the averaged Ψ_{sky} calculated within a 100 m buffer than the Ψ_{sky} calculated for the point location (Lindberg, 2007). A previous LUR study in Hong Kong also demonstrates that it is possible that there are two critical buffers depicting the influence of the same variable at different spatial scales (Shi et al., 2017). Sensitivity tests were performed for each buffer-based variable by using multivariate analysis to understand the sensitivity of the variables' value to different buffer widths and determine the critical buffer width for the variables. In this present study, the critical buffers for each variable were determined by adopting the "A Distance Decay REgression Selection Strategy (ADDRESS)" developed by Su et al. (2009) in their previous LUR modelling studies. A simple linear regression between each buffer-based variable within each buffer width and daytime/nighttime daily averaged T_a was performed for each of the four different seasons in different time periods (2013, 2014, 2015, 2016 and 2013–2016) to check if there is any hidden temporal trend across the study period. It is necessary to confirm whether the correlations are temporally robust when combining with spatial variability. Pearson correlation coefficients (r) were calculated and plotted as a distance-decay curve of distance. Only those buffer-based variables with the highest $|r|$ among all buffers and at the critical positions of the curves were selected as the explanatory variables for further stepwise regression modelling (details of the determination criterion refers to Su et al., 2009). Selecting explanatory variables at the critical buffer from an extensive variables data set avoids iterative regression computations and the over-fitting problem during the stepwise MLR modelling caused by the multicollinearity among too many independent variables (Babyak, 2004).

2.4.2. Stepwise MLR modelling

Stepwise MLR modelling was performed to develop the daytime and nighttime UHI estimation LUR models for different seasons (spring, summer, fall and winter). During the stepwise regression process, the models were initially determined using two different modelling criteria: minimum Akaike information criterion (AICc) and minimum Bayesian information criterion (BIC), in both forward and backward directions using SAS JMP statistical software. The model with the highest adjusted coefficient of determination (\bar{R}^2) was selected. As the results, a total of 10 models were developed (daytime and nighttime, four seasons and annual average). Multicollinearity (the condition when predictor variables are highly correlated with each other) leads to limited independent explanatory capacity and introduces suspicious regressions (Franke, 2010). In the subsequent process, the significant level (measured as p-value) and variance inflation factor (VIF) of each explanatory variables in all these resultant models were checked to

identify multicollinearity issues in all resultant regression models. As a result, variables with p-value > 0.0001 and VIF > 2 were excluded.

2.4.3. Model validation

To evaluate the model performance, we conducted the leave-one-out cross-validation (LOOCV) to compare the difference between the monitored T_a and estimated T_a . The root-mean-square error (RMSE) and the R^2 from the LOOCV (R_{LOOCV}^2) were used to validate the resultant LUR models:

$$RMSE = \sqrt{\frac{1}{n} \sum_{ij=1}^n (T'_{ajj} - T_{ajj})^2}$$

$$R_{LOOCV}^2 = \frac{\sum_{ij=1}^n (T'_{ajj} - \hat{T}_a)^2}{\sum_{ij=1}^n (T_{ajj} - \hat{T}_a)^2}$$

where T_{ajj} is the monitored air temperature at the location i on day j . T'_{ajj} is the estimated air temperature at the location i on day j acquired by using the LUR models. \hat{T}_a is the average value of estimated air temperature T'_{ajj} . n is total amount of data points in the spatiotemporal data set used for LUR modelling.

3. Results

3.1. Critical buffer width of spatial variables

As mentioned, a sensitivity test was performed to determine the critical buffer of spatial variables. Only those spatial variables calculated within its corresponding critical buffers were selected as the explanatory variables for further stepwise regression modelling. Results of the sensitivity test (Table 2) indicate that the critical buffers of these buffer-based spatial predictors remain unchanged across different years. Most of the spatial variables have the same critical buffer width across the day and night (except those spatial variables with diurnal effects). In short, the consistency of critical buffer width among different years implies that the modelling was temporally robust. RES, COM, GOV land use have the same critical buffer of 1500 m while different buffers of 750 m and 400 m have been determined for IND and OPN land use. The building functions and related anthropogenic heat emission in IND land use area are different from other land use types. OPN land use in Hong Kong refers to public open space, urban parks, country parks and other vegetated areas. A feature of OPN areas is that they are beneficial to its surroundings by providing better urban ventilation and vegetation cooling effects. This is also a possible explanation to the similar critical buffer width between OPN and FVC. Two critical buffers have been identified for \bar{h} and BVD . The larger buffer (1500 m) is the same as the RES, COM, GOV land use and that represents the influence of the spatial pattern of land use. The smaller buffer (300 m) of \bar{h} and BVD is the same as the two other geomorphological variables λ_p and $\bar{\lambda}_F$, and that indicates the microscale impacts of building geometry on the local microclimatic condition. These findings are also consistent with the optimal scale of LCZ site determined for the high-density scenario of Hong Kong by a previous local study (Lau et al., 2015). z_0 has been adopted as an indicator of detecting the urban air path (Gál and Sümegegy, 2007; Gál and Unger, 2009) and estimating the spatial variability of UHI (Cardoso et al., 2017; van Hove et al., 2015). The critical buffer identified for z_0 (750 m) by this study could also provide a reference for the experimental design of field measurement of urban climate (Voogt and Oke, 2003). The critical buffer of Ψ_{sky} in the built environment of Hong Kong is 50 m which is smaller than the findings in a previous study (Lindberg, 2007). This implies that the effect of geometrical variable Ψ_{sky} on radiation/energy balance and ventilation is more

Table 2
Critical buffers of the spatial predictors by daytime/nighttime and seasons (unit: m).

Predictors	Spring		Summer		Fall		Winter	
	Daytime	Nighttime	Daytime	Nighttime	Daytime	Nighttime	Daytime	Nighttime
RES	1500	1500	1500	1500	1500	1500	1500	1500
COM	1500	1500	1500	1500	1500	1500	1500	1500
IND	750	750	750	750	750	750	750	750
GOV	1500	1500	1500	1500	1500	1500	1500	1500
OPN	400	400	400	400	400	400	400	400
FVC	400	500	400	500	500	500	500	500
POP	400,2000	400,2000	400,2000	400,2000	400,2000	400,2000	400,2000	400,2000
AADTPT	1000	1000	1000	1000	1000	1000	1000	1000
AADTPG	200,1000	200,1000	200,1000	200,1000	200,1000	200,1000	200,1000	200,1000
\bar{h}	1500	300,1500	1500	300,1500	1500	300,1500	1500	300,1500
λ_p	300	300	300	300	300	300	300	300
BVD	1500	300,1500	1500	300,1500	1500	300,1500	1500	300,1500
Ψ_{sky}	50	50	50	50	50	50	50	50
$\bar{\lambda}_F$	300	300	300	300	300	300	300	300
z_0	750	750	750	750	750	750	750	750

localized (basically at the street canyon scale) in a high-density urban environment.

3.2. The resultant LUR models for UHI estimation

A total of ten models were developed for daytime and night UHI in four different seasons by using the 4-year dataset. The resultant models are shown in Table 3 (regression plots were shown in Fig. 6). All models achieve a high significant level that fulfills the criterion of p-value < 0.0001. The \bar{R}^2 values of these ten models range from 0.562 to 0.762. Most of the models have an \bar{R}^2 of approximately 0.65–0.75 which is a moderately good model performance. The RMSE of nighttime models are generally smaller than daytime models. The results of model cross-validation show that the R^2_{LOOCV} of all models are at a very close level with the corresponding \bar{R}^2 and that validates the reliability of the model performance. In another prior study, the Kriging/Co-kriging geo-interpolation method was used to provide an estimation of the

long-term averaged summertime UHI spatial pattern for Hong Kong (Cai et al., 2017). The Z, NDVI, and Ψ_{sky} were used as covariates during the interpolation process. The prediction accuracy of all interpolation results measured by the R^2_{LOOCV} ranges from 0.574 to 0.614. This accuracy is still lower than the summertime LUR models developed by this present study despite the temporally aggregated data only provide a long-term averaged estimation (without time-series information). The better performance of LUR method indicates that incorporating land use, building variables and sounding data provides better fine-scale spatiotemporal estimation in unmonitored areas.

Basic weather records CLD, Spd and MSLP, as temporal predictors, show in all resultant models. CLD shows in all daytime models and has a strong negative correlation with T_a which is as expected because the amount of cloud determines the incoming solar radiation during daytime. Fewer clouds allow more incoming solar radiation to reach the ground surface and that consequently increases the land surface temperature and then increases daytime air temperature near the ground surface. T_a is negatively correlated with the Spd in all daytime and

Table 3
List of resultant daytime and nighttime UHI estimation models by seasons. All variables fulfill the criterion of p-value < 0.0001 and VIF < 2.

Seasons	Day/night	Resultant UHI estimation models				Model performance evaluation				
		Model structure				R^2	\bar{R}^2	RMSE	R^2_{LOOCV}	p-Value
Spring	Daytime	$-0.701(\text{CLD}) - 0.363(\text{Spd}) - 0.492(\text{MSLP}) + (3.488\text{e-}02)(\text{KINX}) - (5.178\text{e-}03)(\text{Z}) + (5.381\text{e-}07)(\text{RES1500}) + 525.353$				0.685	0.684	2.058	0.684	<0.0001
	Nighttime	$-0.258(\text{Spd}) - 0.510(\text{MSLP}) + (2.097\text{e-}02)(\text{KINX}) - (4.066\text{e-}03)(\text{Z}) - 1.576(\Psi_{sky}0050) - 1.191(\text{FVC0500}) + 539.973$				0.678	0.678	1.864	0.678	<0.0001
Summer	Daytime	$-0.726(\text{CLD}) - (7.886\text{e-}02)(\text{Spd}) + (1.049\text{e-}03)(\text{CAPV}) - (6.823\text{e-}03)(\text{Z}) + (4.328\text{e-}07)(\text{RES1500}) - (1.511\text{e-}02)(z_0750) + 31.942$				0.663	0.663	1.525	0.662	<0.0001
	Nighttime	$-0.335(\text{CLD}) - 0.175(\text{MSLP}) + (8.481\text{e-}04)(\text{CAPV}) - (5.831\text{e-}03)(\text{Z}) + 6.760(\text{BVD1500}) + 1.341(\bar{\lambda}_F0300) + (1.106\text{e-}07)(\text{RES1500}) + 203.835$				0.654	0.654	1.235	0.654	<0.0001
Fall	Daytime	$-0.419(\text{CLD}) - 0.192(\text{Spd}) - 0.367(\text{MSLP}) - 0.248(\text{SHOW}) - (7.157\text{e-}03)(\text{Z}) + (1.802\text{e-}02)(\bar{h}1500) + 402.018$				0.591	0.591	1.970	0.658	<0.0001
	Nighttime	$-0.174(\text{Spd}) - 0.375(\text{MSLP}) - 0.211(\text{SHOW}) - (5.506\text{e-}03)(\text{Z}) - 1.539(\Psi_{sky}0050) - 1.749(\text{FVC0500}) + 408.011$				0.645	0.645	1.955	0.644	<0.0001
Winter	Daytime	$-0.558(\text{CLD}) - 0.289(\text{Spd}) - 0.347(\text{MSLP}) - 0.251(\text{SHOW}) - (6.181\text{e-}03)(\text{Z}) + (2.467\text{e-}02)(\bar{h}1500) + 378.299$				0.591	0.591	2.285	0.590	<0.0001
	Nighttime	$-(4.377\text{e-}02)(\text{CLD}) - 0.168(\text{Spd}) - 0.346(\text{MSLP}) - 0.199(\text{SHOW}) - (5.497\text{e-}03)(\text{Z}) + 15.473(\text{BVD1500}) + 371.640$				0.563	0.562	2.251	0.562	<0.0001
Annual	Daytime	$-0.426(\text{CLD}) - 0.232(\text{Spd}) - 0.700(\text{MSLP}) - (6.455\text{e-}03)(\text{Z}) + (4.231\text{e-}07)(\text{RES1500}) + 735.977$				0.748	0.748	2.890	0.748	<0.0001
	Nighttime	$-0.153(\text{Spd}) - 0.686(\text{MSLP}) - (5.679\text{e-}03)(\text{Z}) + 13.916(\text{BVD1500}) + 717.341$				0.762	0.762	2.705	0.762	<0.0001

nocturnal models because air flows take heat away and cool down the near surface atmosphere. Larger background wind speed contributes to a better condition of urban air ventilation for mitigating the UHI. *MSLP* along with three other sounding indices (*KINX*, *CAPV* and *SHOW*) show in these resultant models as important temporal predictors as well. They depict the meteorological conditions and atmospheric stability which are influential to the UHI. T_a linearly reduces as the altitude increases within the troposphere (for altitude $Z < 11,000$ m). As expected, elevation of the monitoring locations are included in all models and have the regression coefficients basically consistent with the Earth Atmosphere Model (NASA, 2014), as follows:

For $Z < 11000$, $T_a = 15.04 - 0.00649 Z$

where Z is the altitude, T_a is the air temperature.

3.3. LUR spatial mapping of UHI

Based on the resultant models, the long-term averaged spatial mapping of UHI was plotted and shown in Fig. 6. The spatial estimations of UHI were mapped using the spatial resolution of 10 m, the resolution of land use data used in this present study. Regarding the other spatial predictors, as shown in resultant LUR models, two categories of variables - LU/LC and urban surface geomorphometry - are clearly identified as the essential predictors. LU/LC variables, RES1500 (the total area of residential land use within the buffer of 1500 m) and FVC500 (fractional vegetation cover within the buffer of 500 m) are included in resultant models. RES is positively correlated with T_a . It can be seen from the UHI mapping that the spatial distribution of areas with higher T_a is consistent with the RES land use area, especially during summer. The area of residential land use largely reflects the spatial distribution of anthropogenic heat emission (for example, the heat emitted by the summertime air conditioning which is a considerable part of the anthropogenic heat source of Hong Kong) (Giridharan et al., 2005). RES is also positively correlated with the population distribution (which is the reason of the exclusion of spatial variable POP of all resultant models). FVC represents the coverage ratio of urban vegetation/forests which is similar to the NDVI. The difference between FVC and NDVI is that NDVI differentiates between vegetation and bare land based on the remotely sensed signal of near infrared band (of satellite images in the format of raster) while FVC was directly calculated using LU/LC data (in the format of vector data layer in GIS). Therefore, FVC provides more details and has a higher accuracy than NDVI if the LU/LC data is available. In this study, results show that the T_a is negatively correlated with FVC which confirms the cooling effect of urban greenery and its importance in UHI mitigation in high-density Hong Kong (Ng et al., 2012). The spatial pattern of greenery area can be observed on the UHI spatial maps

Building bulks store heat by absorbing shortwave solar radiation during the day and release it by emitting longwave radiation during the night. Larger *BVD* stores more heat than open area during daytime and release more longwave radiation during nighttime. Building geometry with a smaller Ψ_{sky} impedes the longwave radiation back to the sky and traps the heat within the street canyons/gaps between building bulks. The above makes the nighttime cooling rate of ambient air in the urban area much slower than in the rural area, and thus exacerbates the spatial variability in T_a . As a result, a higher T_a remains in the areas with a large *BVD* value and lower Ψ_{sky} . They can be seen in the north of Hong Kong Island and the Kowloon Peninsula. Those built-up areas with a relatively small *BVD* in the New Territories are cooling faster than those large *BVD* areas thus have lower T_a . Unlike our previous LUR models of air quality (Shi et al., 2017), urban traffic variables were not included in the LUR modelling for UHI. This implies that the influence of urban traffic may be less decisive than other predictors despite being one of the most decisive factors of air quality (Shi et al., 2016).

There are still a few clusters of outliers appear in the regression plot. This indicates that there are still potentials of improving UHI LUR models for Hong Kong. Better prediction performance is possible with more informative datasets of variables (e.g. sounding data with a finer temporal scale, building energy consumption records and more detailed data of anthropogenic heat estimation, etc.).

4. Discussion

4.1. Applying LUR in UHI estimation for sub-tropical high-density urban environment

The present study is an attempt to estimate the spatiotemporal UHI pattern in a sub-tropical city with extremely high-density urban environment using LUR modelling. A prior local study has been conducted to associate the short-term meteorological factors with UHI-related mortality in Hong Kong by calculating an UHI index at the geographical tertiary planning units (TPU) level of the city of Hong Kong (Goggins et al., 2012). However, a major limitation of this prior study, which is also shared by some other earlier studies, is that the direct use of meteorological observations from nearby fixed monitoring station may not reflect the actual individual exposure. To overcome above limitation, we provide a fine-scale mapping of spatial variability of T_a using LUR modelling approach in this study, which could provide more accurate information in the representation of the individual exposure condition. LUR method is originally designed for evaluating individual environmental exposure (Kriz et al., 1995). Therefore, identifying UHI hotspots with LUR spatial mapping can provide more information to policy-makers for a more effective health management process than taking each TPU as a whole. The determination of the critical buffer width for each predictor separately is one of the most important procedures of LUR modelling (Hoek et al., 2008). Previous urban climate studies usually analyzed all predictors/variables of the study area based on a grid system with a fixed resolution. However, the critical buffer widths of different spatial predictors may vary due to the complex physical basis of the energy balance and ventilation in the urban microclimate environment. For example, as proved by this present study, the microclimatic effect of Ψ_{sky} on radiation balance and ventilation is more localized than other geomorphometric variables. LUR allows the determination of the spatial scale individually for different predictors and that is helpful in obtaining a better prediction performance. Moreover, the findings and outputs of this present study could be further expanded to other megacities with similar urban scenario (e.g. Guangzhou and Shenzhen, China).

4.2. Estimating spatial pattern of UHI by using geomorphometry as fine-scale spatial predictors

The investigation of fine-scale spatial variability of UHI in an urban environment is an important part of urban planning and policy decision-making, especially for a high-density urban environment because the complicated urban/building morphology significantly changes the microclimatic conditions in urban areas by disturbing the wind field and modifying the energy balance within street canyons. As a result, the microclimatic variability is increased, and thus the UHI pattern is altered. Compared to the previous studies, the spatial mapping of UHI was downscaled by this present study from the TPU level to a very fine spatial scale by parameterizing the urban geomorphometry based on interdisciplinary knowledge.

4.3. LUR UHI modelling as quantitative recommendation for environmental urban design

Urban climate and urban form are interdependent (Eliasson, 1990; Landsberg, 1981). From the viewpoint of urban planning and design, more compact urban forms are commonly thought to be more

sustainable because they save land resources, reduce traffic commuting cost and promote an efficient use of public facilities (Yin et al., 2013). However, a high-density urban environment without appropriate planning/design and management leads to urban environmental degradation (Betanzo, 2007). LUR models developed by this present study enrich the current understanding on the influence of urban design on the urban climatic condition by identifying influential urban design parameters, determining their critical buffers and investigating their quantitative correlations with T_a . For example, as found in the modelling process, $\lambda_{F(0-15m)}$ at the buffer of 300 m has the strongest positive correlation (regression coefficient of 1.341) with T_a during nighttime. This finding indicates that the T_a of a specific location is strongly influenced by the horizontal permeability of podium layer within its surrounding of 300 m due to the impact of the building geometrical permeability on ventilation. An increase of 20,000m² in building frontal area is associated with a 0.5 °C increase in T_a . Simply speaking, designing and constructing one single large building without proper consideration on urban ventilation may lead to an increase of 0.5 °C in UHI intensity of the whole neighborhood. Such information could substantially enrich the current urban design guideline – Chapter 11 of the Hong Kong Planning Standards and Guidelines (HKPSG) (PlanD, 2005) and help with the UHI mitigation.

5. Conclusion

Assessing the exposure to urban environmental heat is essential. The fine-scale estimation of the spatiotemporal pattern of UHI is urgently needed for heat exposure assessment and public health management. LUR is a promising method of predicting environmental spatiotemporal variability and estimating human exposure. In this present study, we modelled the fine-scale spatiotemporal UHI pattern using the LUR method with land use, building variables and sounding data. Our resultant spatiotemporal LUR models provide a daily-resolved estimation of air temperature (for both the daytime and the nighttime) at a very fine spatial scale (of a 10 m resolution), which provide a robust basis for heat exposure assessment. The study outputs also enable the integration of environmental consideration into urban environmental planning policy for a better quality of living environment. The findings of this present study could be further expanded to other cities with a similar densely-populated urban scenario.

Author contributions

The manuscript was written through contributions of all authors. All authors have given approval to the final version of the manuscript. The authors declare no competing financial interest.

Acknowledgment

This research is supported by the General Research Funds (GRF Project Number: 14610717, “Developing urban planning optimization strategies for improving air quality in compact cities using geo-spatial modelling based on in-situ data” and GRF Project Number: 14611517, “Climatic-responsive planning and action for mitigating heat-related health risk at community level in high density cities – A Case of Hong Kong”) from the Research Grants Council (RGC) of Hong Kong. The authors wish to thank the Department of Atmospheric Science, University of Wyoming, especially Dr. Larry Oolman, for providing the atmospheric sounding indices data (Station No. 45004). The authors would like to thank Professor Kevin Ka-Lun Lau, Prof Chao Ren and Ms. Ada Lee of the Chinese University of Hong Kong and Dr. Derrick Ho of the Hong Kong Polytechnic University for their suggestion and help on this paper. The authors deeply thank reviewers for their insightful comments, feedbacks and constructive suggestions, recommendations on our research work. The authors also want to appreciate editors for their patient and meticulous work for our manuscript.

Reference

- Anderson, B.G., Bell, M.L., 2009. Weather-related mortality: how heat, cold, and heat waves affect mortality in the United States. *Epidemiology* 20, 205.
- Arnfield, A.J., 2003. Two decades of urban climate research: a review of turbulence, exchanges of energy and water, and the urban heat island. *Int. J. Climatol.* 23, 1–26.
- Babyak, M.A., 2004. What you see may not be what you get: a brief, nontechnical introduction to overfitting in regression-type models. *Psychosom. Med.* 66, 411–421.
- Betanzo, M., 2007. Pros and cons of high density urban environments. *Build* 39–40 (April/May).
- Bottyán, Z., Unger, J., 2002. The Role of Land-use Parameters in the Spatial Development of Urban Heat Island in Szeged, Hungary.
- Buechley, R.W., Van Bruggen, J., Truppi, L.E., 1972. Heat island = death island? *Environ. Res.* 5, 85–92.
- Cai, M., Ren, C., Lau, K.K.-L., Xu, Y., 2017. Spatial analysis on intra-urban temperature variation under extreme hot weather by incorporating urban planning and environmental parameters: a pilot study from Hong Kong. *Passive Low Energy Architecture (PLEA) 2017*, Edinburgh, Scotland.
- Cardoso, R., Dorigon, L., Teixeira, D., Amorim, M., 2017. Assessment of urban heat islands in small- and mid-sized cities in Brazil. *Climate* 5, 14.
- Chau, P.H., Chan, K.C., Woo, J., 2009. Hot weather warning might help to reduce elderly mortality in Hong Kong. *Int. J. Biometeorol.* 53, 461.
- Chen, L., Ng, E., An, X., Ren, C., Lee, M., Wang, U., et al., 2012. Sky view factor analysis of street canyons and its implications for daytime intra-urban air temperature differentials in high-rise, high-density urban areas of Hong Kong: a GIS-based simulation approach. *Int. J. Climatol.* 32, 121–136.
- Chin, P.C., 1986. *Climate and Weather*. In: Chiu, T.N., So, C., Catt, P. (Eds.), *A Geography of Hong Kong*. Oxford University Press HK, New York.
- Clarke, J.F., 1972. Some effects of the urban structure on heat mortality. *Environ. Res.* 5, 93–104.
- Dozier, J., Frew, J., 1990. Rapid calculation of terrain parameters for radiation modeling from digital elevation data. *IEEE Trans. Geosci. Remote Sens.* 28, 963–969.
- Eliasson, L., 1990. Urban geometry, surface temperature and air temperature. *Energ. Buildings* 15, 141–145.
- Fan, H., Sailor, D.J., 2005. Modeling the impacts of anthropogenic heating on the urban climate of Philadelphia: a comparison of implementations in two PBL schemes. *Atmos. Environ.* 39, 73–84.
- Franke, G.R., 2010. *Multicollinearity*. Wiley International Encyclopedia of Marketing. John Wiley & Sons, Ltd.
- Gál, T., Sümeghy, Z., 2007. Mapping the roughness parameters in a large urban area for urban climate applications. *Acta Climatol. Chorologica* 40–41.
- Gál, T., Unger, J., 2009. Detection of ventilation paths using high-resolution roughness parameter mapping in a large urban area. *Build. Environ.* 44, 198–206.
- Gallo, K.P., Tarpley, J.D., McNab, A.L., Karl, T.R., 1995. Assessment of urban heat islands: a satellite perspective. *Atmos. Res.* 37, 37–43.
- Giridharan, R., Lau, S.S.Y., Ganesan, S., 2005. Nocturnal heat island effect in urban residential developments of Hong Kong. *Energ. Buildings* 37, 964–971.
- Givoni, B., 1998. *Climate Considerations in Building and Urban Design*. John Wiley & Sons, New York.
- Goggins, W.B., Chan, E.Y.Y., Ng, E., Ren, C., Chen, L., 2012. Effect modification of the association between short-term meteorological factors and mortality by urban Heat Islands in Hong Kong. *PLoS One* 7, e38551.
- Hillevi, U., Deliang, C., 1999. Influence of geographical factors and meteorological variables on nocturnal urban-park temperature differences—a case study of summer 1995 in Göteborg, Sweden. *Clim. Res.* 13, 125–139.
- HKTD, 2016. *The Annual Traffic Census 2015*. Transport Department, HKSAR, Hong Kong.
- Hoek, G., Beelen, R., de Hoogh, K., Vienneau, D., Gulliver, J., Fischer, P., et al., 2008. A review of land-use regression models to assess spatial variation of outdoor air pollution. *Atmos. Environ.* 42, 7561–7578.
- Katzschner, L., Mülder, J., 2008. Regional climatic mapping as a tool for sustainable development. *J. Environ. Manag.* 87, 262–267.
- Kloog, I., Nordio, F., Coull, B.A., Schwartz, J., 2012. Incorporating local land use regression and satellite aerosol optical depth in a hybrid model of spatiotemporal PM_{2.5} exposures in the mid-Atlantic States. *Environ. Sci. Technol.* 46, 11913–11921.
- Kotharkar, R., Bagade, A., 2017. Local climate zone classification for Indian cities: a case study of Nagpur. *Urban Climate* <http://dx.doi.org/10.1016/j.uclim.2017.03.003>.
- Kriz, B., Bobak, M., Martuzzi, M., Briggs, D., Livesley, E., Lebre, E., et al., 1995. *Respiratory Health in the SAVIAH Study*.
- Landsberg, H.E., 1981. *The Urban Climate*. Vol. 28. Academic press, London.
- Lau, K.K.-L., Ren, C., Shi, Y., Zheng, V., Yim, S., Lai, D., 2015. Determining the optimal size of local climate zones for spatial mapping in high-density cities. 9th International Conference on Urban Climate jointly with 12th Symposium on the Urban Environment. International Association for Urban Climate (IAUC) and American Meteorological Society (AMS), Toulouse, France.
- Lecante, F., Bouyer, J., Claverie, R., Pétrissans, M., 2015. Using local climate zone scheme for UHI assessment: evaluation of the method using mobile measurements. *Build. Environ.* 83, 39–49.
- Lee, D.O., 1979. The influence of atmospheric stability and the urban heat island on urban-rural wind speed differences. *Atmos. Environ.* 1967 (13), 1175–1180.
- Li, D., Bou-Zeid, E., 2013. Synergistic interactions between urban heat islands and heat waves: the impact in cities is larger than the sum of its parts. *J. Appl. Meteorol. Climatol.* 52, 2051–2064.
- Lindberg, F., 2007. Modelling the urban climate using a local governmental geo-database. *Meteorol. Appl.* 14, 263–273.
- Liu, L., Zhang, Y., 2011. Urban heat island analysis using the Landsat TM data and ASTER data: a case study in Hong Kong. *Remote Sens.* 3, 1535.

- Meehl, G.A., Tebaldi, C., 2004. More intense, more frequent, and longer lasting heat waves in the 21st century. *Science* 305, 994–997.
- NASA, 2014. Earth Atmosphere Model - English Units. In: Benson T, Editor. 2017, USA.
- Ng, E., Ren, C., 2015. The Urban Climatic map: A Methodology for Sustainable Urban Planning: Routledge.
- Ng, E., Chen, L., Wang, Y., Yuan, C., 2012. A study on the cooling effects of greening in a high-density city: an experience from Hong Kong. *Build. Environ.* 47, 256–271.
- Nichol, J., Wong, M.S., 2005. Modeling urban environmental quality in a tropical city. *Landscape Urban Plan.* 73, 49–58.
- Oke, T.R., 1973. City size and the urban heat island. *Atmos. Environ.* 1967 (7), 769–779.
- Oke, T.R., 1982. The energetic basis of the urban heat island. *Q. J. R. Meteorol. Soc.* 108, 1–24.
- Patz, J.A., Campbell-Lendrum, D., Holloway, T., Foley, J.A., 2005. Impact of regional climate change on human health. *Nature* 438, 310–317.
- PlanD, 2005. Hong Kong Planning Standards and Guidelines (HKPSG) Hong Kong Planning Department, Hong Kong, PRC.
- Rizwan, A.M., Dennis, L.Y.C., Liu, C., 2008. A review on the generation, determination and mitigation of urban heat island. *J. Environ. Sci.* 20, 120–128.
- Roth, M., Oke, T., Emery, W., 1989. Satellite-derived urban heat islands from three coastal cities and the utilization of such data in urban climatology. *Int. J. Remote Sens.* 10, 1699–1720.
- Ryan, P.H., LeMasters, G.K., 2007. A review of land-use regression models for characterizing intraurban air pollution exposure. *Inhal. Toxicol.* 19, 127–133.
- Sailor, D.J., Lu, L., 2004. A top-down methodology for developing diurnal and seasonal anthropogenic heating profiles for urban areas. *Atmos. Environ.* 38, 2737–2748.
- Saraswat, A., Apte, J.S., Kandlikar, M., Brauer, M., Henderson, S.B., Marshall, J.D., 2013. Spatiotemporal land use regression models of fine, ultrafine, and black carbon particulate matter in New Delhi, India. *Environ. Sci. Technol.* 47, 12903–12911.
- Shi, Y., Lau, K.K.-L., Ng, E., 2016. Developing street-level PM_{2.5} and PM₁₀ land use regression models in high-density Hong Kong with urban morphological factors. *Environ. Sci. Technol.* 50, 8178–8187.
- Shi, Y., Lau, K.K.-L., Ng, E., 2017. Incorporating wind availability into land use regression modelling of air quality in mountainous high-density urban environment. *Environ. Res.* 157, 17–29.
- Siu, L.W., Hart, M.A., 2013. Quantifying urban heat island intensity in Hong Kong SAR, China. *Environ. Monit. Assess.* 185, 4383–4398.
- Su, J.G., Jerrett, M., Beckerman, B., Wilhelm, M., Ghosh, J.K., Ritz, B., 2009. Predicting traffic-related air pollution in Los Angeles using a distance decay regression selection strategy. *Environ. Res.* 109, 657–670.
- Svensson, M.K., 2004. Sky view factor analysis—implications for urban air temperature differences. *Meteorol. Appl.* 11, 201–211.
- Taha, H., 1997. Urban climates and heat islands: albedo, evapotranspiration, and anthropogenic heat. *Energ. Buildings* 25, 99–103.
- Tomlinson, C.J., Chapman, L., Thornes, J.E., Baker, C., 2011. Remote sensing land surface temperature for meteorology and climatology: a review. *Meteorol. Appl.* 18, 296–306.
- Unger, J., 2004. Intra-urban relationship between surface geometry and urban heat island: review and new approach. *Clim. Res.* 27, 253–264.
- van Hove, L.W.A., Jacobs, C.M.J., Heusinkveld, B.G., Elbers, J.A., van Driel, B.L., Holtslag, A.A.M., 2015. Temporal and spatial variability of urban heat island and thermal comfort within the Rotterdam agglomeration. *Build. Environ.* 83, 91–103.
- Voogt, J.A., Oke, T.R., 2003. Thermal remote sensing of urban climates. *Remote Sens. Environ.* 86, 370–384.
- WHO, 2003. Climate Change and Human Health: Risks and Responses: Summary. World Health Organization. Dept. of Protection of the Human Environment, Geneva.
- Xie, D., Liu, Y., Chen, J., 2011. Mapping urban environmental noise: a land use regression method. *Environ. Sci. Technol.* 45, 7358–7364.
- Yan, Y.Y., 2000. The influence of weather on human mortality in Hong Kong. *Soc. Sci. Med.* 50, 419–427.
- Yin, Y., Mizokami, S., Maruyama, T., 2013. An analysis of the influence of urban form on energy consumption by individual consumption behaviors from a microeconomic viewpoint. *Energ. Policy* 61, 909–919.
- Yuan, F., Bauer, M.E., 2007. Comparison of impervious surface area and normalized difference vegetation index as indicators of surface urban heat island effects in Landsat imagery. *Remote Sens. Environ.* 106, 375–386.
- Zhang, Y., Odeh, I.O.A., Han, C., 2009. Bi-temporal characterization of land surface temperature in relation to impervious surface area, NDVI and NDBI, using a sub-pixel image analysis. *Int. J. Appl. Earth Obs. Geoinf.* 11, 256–264.
- Zhou, W., Ji, S., Chen, T.-H., Hou, Y., Zhang, K., 2014a. The 2011 heat wave in Greater Houston: effects of land use on temperature. *Environ. Res.* 135, 81–87.
- Zhou, W., Qian, Y., Li, X., Li, W., Han, L., 2014b. Relationships between land cover and the surface urban heat island: seasonal variability and effects of spatial and thematic resolution of land cover data on predicting land surface temperatures. *Landscape Ecol.* 29, 153–167.